Hydrol. Earth Syst. Sci. Discuss., 9, 2511–2539, 2012
www.hydrol-earth-syst-sci-discuss.net/9/2511/2012/
doi:10.5194/hessd-9-2511-2012

Hydrology and Earth System Sciences Discussions

Assessment of shallow subsurface characterization with non-invasive geophysical methods at the intermediate hill-slope scale

S. Popp, D. Altdorff, and P. Dietrich

UFZ, Helmholtz Centre for Environmental Research,
Department Monitoring and Exploration Technologies, Leipzig, Germany

Received: 26 January 2012 – Accepted: 14 February 2012 – Published: 24 February 2012

Correspondence to: S. Popp (steffen.popp@ufz.de)

Published by Copernicus Publications on behalf of the European Geosciences Union.

Abstract

Hill-slopes of several hectares in size represent a difficult scale for subsurface characterization, as these landscape units are well beyond the scope of traditional point-scale techniques. By means of electromagnetic induction (EMI) and gamma-ray spectroscopy, spatially distributed soil proxy data were collected from a heterogeneous hill-slope site. Results of repeated EMI mapping using the EM38DD showed that soil electrical conductivity (EC_a) is highly variable at both temporal and spatial scales. Calibration of the integral EC_a signal to soil moisture is hampered by the ambiguous response of EMI to the clay-rich hill-slope underground. Given a stationarity signal of geologic background, temporal changes of EC_a are attributable to relative soil-moisture dynamic. Gamma-ray results were obtained during a single survey, along with EM measurements and selected soil sampling. In contrast to EC_a, a noticeable correlation between Total Count and K emission data and soil-water content seemed to be present. Relevant proxy variables from both methods were used for *k*-means clustering in order to distinguish between hill-slope areas with different soil conditions. As a result, we obtained a suitable partition of hill-slope that was comparable with a previously obtained zonation model based on ecological factors.

1 Introduction

Exploration of near-surface ground on hill-slopes still poses a significant challenge in hydrological or natural-hazard sciences due to subsurface heterogeneity at intermediate landscape scales (commonly less than one square kilometer). Point measurements, e.g. in situ soil-moisture determination by specific probes or sediment sampling for laboratory analyses provide quantitative data, however, only from a very limited area or volume of the subsurface. As point measures are relatively costly and time consuming, sampling is often limited to a few selected points. Scaling up point data in order to infer information for the entire hill-slope area is problematic, with respect to the heterogeneous underground.

HESSD
9, 2511–2539, 2012

Geophysical methods provide the possibility of gathering spatially distributed data, and are thus nowadays being increasingly applied for landscape characterization (Schrott and Sass, 2008; Van Damm, 2012). Besides structural prospecting in hill-slope and landslide studies in addition to geological investigations (e.g. Chambers et al., 2010; Sass et al., 2008), geophysical techniques are widely-used for the spatial mapping of physical variables, e.g. electrical conductivity (EC). EC is a key parameter for the description of near-surface ground due to its close relationship to soil and hydrological properties (Caroll and Oliver, 2005; Corwin and Lesch, 2003; Ewing and Hunt, 2006; Brevik et al., 2006). Ground-based electromagnetic induction (EMI) methods have proven an efficient technique for rapid and area-wide mapping of soil EC. EMI measure a depth-weighted average of the soil electrical conductivity to a specific depth, the so-called apparent electrical conductivity (EC_a in milli Siemens per meter, $mS\,m^{-1}$). Thereby, EC_a is a sum parameter and predominately influenced by the volumetric water content, salinity, the types and amount of clay minerals, porosity, and soil temperature (McNeil, 1980).

Despite the multiple factors influencing EC_a, previous benchmark studies by Kachanoski et al. (1988, 1990) and Sheets and Hendrickx (1995) have shown that EMI can potentially be used for soil-moisture mapping. By using the EM31 and EM38 sensors (Geonics Ltd., ON, Canada), the studies showed that the EC_a signal could explain most shallow subsurface variations of soil moisture. Similarly, Sherlock and McDonnell (2003) and Buchanan and Triantafilis (2009) used EMI for mapping of the distribution of water table depth. Other studies utilize the relationships of the EC_a signal for the detection of clay layers (e.g. Cockx et al., 2007) or the estimation of soil textural features (e.g. Domsch and Giebel, 2004). However, most of the studies that investigated spatial soil-moisture patterns were conducted in flat, easily accessible, relatively homogeneous and rather small areas (ranging between 0.05 and 3.5 ha in size). Additionally, a considerable effort was applied for the determination of soil-water contents (e.g. Reedy and Scanlon, 2003; Martinez et al., 2010). For the hill-slope scale, we are aware of only one study that uses EMI for the investigation of soil-moisture patterns and does so at a relatively small test site of less than 0.1 ha size (Tromp-van Meerveld and McDonnell, 2009). By means of performing extended soil-moisture monitoring, the aforementioned authors achieved a reliable correlation for predicting soil moisture with EC_a values, however, only by using individual relationships determined at each of the sixty-four measuring points. The use of one (master) relationship for the calculation of water contents resulted in a smoothed soil-moisture pattern that did not represent the observed soil-moisture pattern very well. This study, even with promising results, illustrates the main drawback of EMI application in sloped areas with a heterogeneous subsurface – the challenge presented in gaining a reliable calibration of the EC_a signal to soil moisture or other soil state variables. The effort required for ground truthing of EC_a values is likely to increase significantly and may become ultimately unfeasible on larger field sizes in heterogeneous areas. Thus, other approaches for extracting subsurface information from larger areas should be adopted.

In the present study, we combined EMI with gamma-ray spectroscopy for characterizing shallow subsurface heterogeneity in the headwaters of a mountainous catchment. Gamma-ray spectrometry serves as an additional tool for mapping near-surface soil properties without complex data inversion procedures. The method measures gamma-ray radiation emitted from the natural decay of radioactive elements that are present in rocks and soils (e.g. Minty, 1997; Dickson and Scott, 1997; Wilford et al., 1997). Both the concentration and the ratio of specific radioactive elements can give information on soil properties such as surface texture (e.g. Taylor et al., 2002), clay content (e.g. Pracilio et al., 2006), or soil-moisture patterns (e.g. Carroll, 1981; Grasty, 1997). Both EMI and gamma-ray methods were conducted at a 13-ha sized hill-slope area, which is characterized by a low creeping movement. The mobility of the movement is predominantly controlled by hydrological processes such as pore-water pressure fluctuations and the variable weight of soil due to variable water contents (Lindenmaier et al., 2005; Wienhöfer et al., 2011). Thus, knowledge of spatially distributed soil-water pattern and relevant soil-structures is a prerequisite for e.g. modeling landslide behavior.

HESSD
9, 2511–2539, 2012

The goal of this study is the reasonable exploration and characterization of the hill-slope subsurface based on mapping of soil proxy values. Thereby we try to minimize the need for invasive measures because soil sampling and soil testing are commonly critical points due to time and cost constraints. Therefore the number of soil samples is restricted to a manageable quantity of less than 20 samples, which are used for evaluation of both methods under site-specific condition. Following the qualitative approach, we target at a spatially meaningful partitioning of the heterogeneous subsurface as basis for further detailed investigations, and examine the geophysical-based results with a previously obtained hill-slope zonation from hydrological and soil-survey studies.

2 Material and methods

2.1 Study site

The study area Heumöser (Fig. 1) is located near the Rhine River valley in the western Vorarlberg Alps, Austria, around 10 km south of city of Dornbirn and 0.5 km south of the village of Ebnit (47°21′0.0″ N, 9°44′46.6″ E). The Heumöser belongs to the head of a steep mountainous catchment and covers 0.95 km^2 with an extension of 1800 and 500 m in east-west and north-south directions, respectively. The bedrocks that underlie and surround the Heumöser slope are sedimentary marlstones from the Upper Cretaceous, belonging to the Alpine Helvetic zone (Lindenmaier et al., 2005). Unweathered marlstones are a mixture of calcite, quartz, and clay minerals. The cover sediments, which reach a thickness of up to 40 m, are described as loamy scree and glacial till with variable proportions of calcite (up to 40 %), quartz (25–40 %), and clay (up to 30 %) (Schneider, 1999). The water content of these sediments ranges from 20 to 30 %. In soil profiles, water content and proportions of clay can vary, and in particular the water content can be significantly increased.

The Heumöser is a slow moving landslide with surface movement rates of 0.01 to 0.25 $m\,yr^{-1}$ (Depenthal and Schmidt, 2003). Inclinometer measurements in boreholes

(Fig. 1) identified subsurface deformation along a shear zone between 7.5 and 8.5 m depths in KB3 (Schneider, 1999), and between 10.5 and 12.0 m depths in HH4 (Wienhöfer et al., 2009).

The geophysical surveys for shallow subsurface exploration focus on the accessible meadow areas in the middle and north-western parts of the Heumöser (Fig. 1) between 1039 and 1233 m altitude. This area covers approximately 13 ha with maximum extension of 1030 and 300 m in east-west and north-south directions, respectively. The topography is highly variable, with relatively steep and hummocky terrain in the west with an average slope angle of 19.5°, and a rather plane surface in the east. The Heumöser is subdivided into four so-called hydrotopes or hydrologic response units (HRU), according to long-term average soil moisture patterns found in detailed botanic and hydropedologic mapping (Lindenmaier et al., 2005; Wienhöfer et al., 2009). The investigated slope area belongs to HRU 2 and 3, which are generally characterized by very moist to very wet topsoil conditions in plane areas, and dryer conditions in bulging areas (Fig. 1).

2.2 Electromagnetic measurements

We conducted two electromagnetic mapping surveys at the beginning of May and in the middle of June 2011. The first field survey was performed under highly water-saturated soil conditions, shortly after all snow had fully melted. The second measurement was carried out one month later when the subsurface was expected to be less water saturated, in order to detect changes in soil electrical conductivity.

We used the EM38DD electromagnetic induction sensor (Geonics Ltd., ON, Canada) for mapping soil electrical conductivity. The sensor operates in the frequency domain at fixed coil spacing of 1 m. An alternating current at a specific frequency in the transmitter coil induces a primary electromagnetic field that propagates through the subsurface and generates a secondary magnetic field. The receiver coil detects the primary and secondary magnetic fields at the surface. The ratio of these two readings gives the depth-weighted apparent electrical conductivity (EC_a in $mS\,m^{-1}$). The EM38DD

Discussion Paper | Discussion Paper | Discussion Paper | Discussion Paper |
HESSD
9, 2511–2539, 2012
Assessment of shallow subsurface characterization
S. Popp et al.

consist of two EM38 units fixed perpendicularly to each other, which results in two simultaneous conductivity readings with different depth response profiles. The sensor in vertical orientation (EC_v) receives its major influence from the shallow subsoil with a common exploration depth of up to 1.5 m. The horizontally orientated sensor (EC_h) is most sensitive to the uppermost topsoil and reaches depths of 0.75 m.

The two field surveys were organized differently. In May 2011, EC_a proximal sensing was performed "on-the-go", with an average line spacing of 15 m. In June 2011, EC_a proximal sensing was conducted as point measurements at 327 locations with additional gamma-ray spectroscopy and soil sampling taking place at 18 locations (Fig. 2a). In all surveys, spatial reference of sampling points was determined by an external D-GPS system (Leica 1200) connected to the EMI recording unit. Before surveying, the EM38DD sensor was calibrated at the same point on the site according to the user manual at the beginning of each field site measurement day. Additionally, we recorded a reference profile repeatedly both before and in between the measurements in order to check data quality and serviceability of the instrument.

To avoid interferences to EMI response whilst surveying, an appropriate distance from the metallic masts of the ski lift has to be maintained. Further outliers in the EC_a data set which occurred as a result of non-visible EMI interferences were removed, while data analysis was performed by applying a filter that only allows for data within the triple of the root mean square deviation to be considered. Since soil electrical conductivity can vary due to changes in soil temperature, we standardized the field apparent conductivity values to an equivalent conductivity at a reference temperature (25 °C) using measured soil temperature and a conversion function given by Sheets and Hendrickx (1995) and Reedy and Scanlon (2003):

$$EC_{25} = EC_a \left(0.4779 + 1.3801 e^{\left(\frac{-T}{25.654}\right)}\right) \quad (1)$$

where EC_{25} is the temperature corrected apparent conductivity, EC_a is the measured apparent conductivity ($mS\,m^{-1}$), and T is the soil temperature (°C). Soil temperature measured at the soil surface at a 10-cm depth was in average 8.5 °C and 15 °C in

HESSD
9, 2511–2539, 2012

May and June, respectively. When discussing apparent conductivity in the following sections, we always refer to the temperature corrected values. Maps of shallow subsurface apparent conductivity were obtained by variogram analysis and ordinary kriging interpolation, using a 20-m grid.

2.3 Gamma ray spectroscopy

For proximal gamma-ray sensing, we used the portable *Exploranium* GR256 gamma-ray spectrometer with a 0.35-l thallium activated NaI crystal detector (Exploranium, Ontario, Canada). The gamma sensor detects the gamma radiation of variable energies that is emitted by the natural decay of radioactive elements present in rocks and soils. Thereby, about 90 % of the gamma radiation measured at the surface emanates from the upper 30 cm, and about 50 % comes from the top 10 cm (e.g. Cook et al., 1996; IAEA, 2003).

At the Heumöser, gamma-ray measurements were taken at 327 points by placing the detector on the ground surface. A single measurement took 60 s to complete, which was evaluated by test measurements to be an adequate time interval, with regards to signal stability and the number of measuring points. According to the default settings of the spectrometer, gamma radiation was measured in four energy windows, so-called "regions of interest" (ROI), with specific energy ranges that allow for the detection of total number of decays (Total Count), as well as of potassium-40 (K), uranium-238 (U), and thorium-232 (Th) (cf. Viscarra Rossel et al., 2007). Individual gamma data and local variograms were used for kriging interpolation on a 20-m grid analogue to the EC_a values.

HESSD
9, 2511–2539, 2012

Title Page
Abstract Introduction
Conclusions References
Tables Figures
◂◂ ▸▸
◂ ▸
Back Close
Full Screen / Esc
Printer-friendly Version
Interactive Discussion

3 Results and discussion

3.1 Apparent electromagnetic conductivity measurements

Soil electrical conductivity is highly variable on the hill-slope. The overall range of EC_a is between 1 and 60 mS m^{-1}, with coefficients of variation (CV) in the range of 17 to 30 % for individual EC_h and EC_v measurements (Table 1). Results of kriging interpolation reveal defined spatial pattern of EC_a (Fig. 2b, c) that can be explained in a site-specific context.

In May, apparent conductivity shows a significant vertical gradient from a very conductive top soil (EC_h response) towards less conductive deeper layers (EC_v response) in most parts of the hill-slope. While zones of low EC_v readings (<20 mS m^{-1}) in the steeper eastern hill-slope area can be partly attributed to near-surface bed rock (<1-m deep), the high EC_h readings are very likely linked to the high water content of the top soil after snowmelt. In June, vertical graduation of EC_a was less pronounced due to decreased conductivity of the top soil. Both the EC_h and EC_v readings can be used for the calculation of a profile ratio (PR), as an indication for the heterogeneity of the soil column, defined as: $PR = EC_h/EC_v$ (Corwin et al., 2003; Cockx et al., 2007). A PR close to 1 points to a uniform profile of soil electrical conditions. A $PR < 1$ indicates a more conductive subsoil relative to the topsoil, and a $PR > 1$ indicates a conductive topsoil and decreasing conductivity with depth. Figure 2d shows the areas of the hill-slope with different vertical graduations. In May, the majority of the hill-slope subsurface is dominated by conductive topsoil conditions ($PR >> 1$). The situation had changed in June, where relatively uniform soil conditions ($PR \sim 1$) with intermediate electrical conductivities prevailed over nearly half of the hill-slope area.

To assess the relationship between soil water and EC_a response at the site, gravimetric water content from 18 soil samples was determined in the laboratory. Soil samples were collected from depths between 10 and 40 cm, along with EC_a point measurements in June. The location of soil samples is shown in Fig. 2a. Gravimetric soil-water content ranges from 25 to 82 % relative to the dry weight of the soil sample. Highest

HESSD
9, 2511–2539, 2012

values of 62 to 82 % were determined at four organic-rich soil samples located in the flat eastern part of the hill-slope, while most of the samples show water contents in the range of 25 to 48 %. As shown in Fig. 3, there exists no definitive correlation between soil-water content and EC_a at the time of sampling, neither with EC_h nor with EC_v. The suggested, but insignificant, correlation of EC_h is obviously caused by the exceptionally high water contents of few organic-rich soil-samples. Evidently, EC_a at the study site seems not to solely depending upon water saturation, but also on soil structure and mineral content. At the Heumöser, soils are described as gley and stagno gley soils, or silty clay to silty loams according to the US soil taxonomy (Lindenmaier et al., 2005). Relatively high proportions of clayey and silty material, which were also evident in the recovered soil samples, are supposed to contribute significantly to the integral signal of soil electrical conductivity. This issue can obviously result in relatively low EC_a readings for organic soils even though the soil-water content is high, and vice versa, in relatively high EC_a values for clayey soils with lower gravimetric soil-water content. Hence, a distinction between temporally variable soil moisture and the geological background is not possible based on a single EMI mapping survey.

However, given that the type and amount of clay minerals, soil structure, and ionization of the soil moisture do not change over the considered period of time, EC_a variations in repeated measurements are presumably linked to relative changes in soil moisture (Robinson et al., 2009, 2012; Martinez et al., 2010). The lower apparent conductivity of near-surface EC_h response in June can thus be associated with lower soil moisture compared to the topsoil conditions in May. In contrast, the less pronounced variability of EC_v readings can in general be explained by the stagnic properties of the silty and clayey subsoil. This interpretation is reinforced by findings from a TDR profile measurements carried out at the hill-slope, where almost no soil-moisture variation occurred in the deeper subsoil (80-cm depth), while data at a 20-cm depth shows around 10 % of seasonal variation in soil moisture (Lindenmaier et al., 2005).

HESSD
9, 2511–2539, 2012

3.2 Gamma-ray survey

Gamma-ray emission is relatively low at the hill-slope with maximum values of 583, 83, and 125 counts per 60 s for K, Th, and U (Table 1). Total Count, which is the sum signal of all radioactive emissions, reaches maximum 2537 counts per 60 s. Despite the low emission rates and relatively minor data ranges, the variability of gamma-ray flux data is high and more pronounced at smaller spatial scales compared to EMI. For example, gamma-ray flux between two neighboring sampling points can differ significantly from each other due to the small support volume of the gamma-ray method and changing subsurface microstructures. As a result, coefficients of variation are in the range of 28 and 38 % (Table 1). However, regardless of the pronounced small-scale variability, gamma-ray emission data show definite spatial pattern at the hill-slope scale similar to those of EC_a.

As shown by the maps obtained from kriging interpolation, highest emission values are concentrated in the north-western part of the slope (Fig. 4). According to the situation in field, these high radioactive emission values are very likely caused by allochthonous material from a backfill on the ski trail. The majority of emission values (around 90 % of data) for Total Count and K is below 1700 and 400 counts per 60 s, respectively, indicating shallow subsurface concentrations lower than 1 ppm (U equivalent) for Total Count and lower than 0.5 % for K. When we consider the mineral composition of loamy scree sediments of the subsoil, consisting among others of K-bearing minerals illite and muscovite (up to 10 %), feldspar (up to 3 %), and up to 20 % swell-capable clay minerals (Schneider, 1999) with their ability to adsorb released potassium, one would expect much higher emission values. For example, soils composed of loamy textured till with silty to clayey cover layers in west-central Canada exhibit K levels of 1.3 to 1.6 % (Kiss et al., 1988), or Australian soils on shale bed rock exhibit K concentrations in the range of 0.7 to 3.0 % (Dickson and Scott, 1997).

Thus, the low radioactive emissions at the Heumöser are very likely the consequence of high soil-water contents. Soil moisture increases the bulk density of soils and thus

HESSD
9, 2511–2539, 2012

the attenuation of gamma radiation. The signal attenuation is increased by approximately 1 % for each increment of 1 % volumetric water content (Cook et al., 1996). When cross-plotting the obtained gravimetric water contents and gamma-ray data, a notably negative correlation becomes evident with Total Count and K radioactivity measurements (Fig. 5). The lower the soil-water content, the higher the gamma-ray emission. This attenuation effect of gamma-ray fluxes, in particular from K and Th with increasing soil moisture, is known from results achieved by airborne gamma-ray measurements (e.g. Carroll, 1981; Grasty, 1997). The latter named authors utilized this relationship for quantifying soil-water contents based on repeatedly measured gamma-ray emission flux under dry and wet soil conditions. Repeated measuring results have not been obtained from the site, however, the snap shot of spatial gamma-ray flux allows for a first assessment of relative water contents of the topsoil (relatively wet-moist-dry) based on the correlation shown in Fig. 5.

3.3 Hill-slope characterization and partitioning

The ambiguous relationship between electrical conductivity and gamma-ray flux and the highly heterogeneous soil properties at the Heumöser hamper the straightforward characterization of subsurface structures or soil state variables by means of EMI or gamma-ray spectroscopy. Therefore we use selected variables from both methods for a joint analysis based on a cluster algorithm in order to identify zones of similar soil conditions. The so-called zonal approach (based on e.g. k-means or fuzzy c-means clustering) has become a common tool in geophysical data analysis for delineating subsurface structures and estimating petrophysical parameters (e.g. Tronicke et al., 2004; Dietrich and Tronicke, 2009; Paasche et al., 2010; Altdorff and Dietrich, 2012). We chose k-means clustering because of its simple performance and robust results, using the software *Systat*. Input variables were EC_h data from both May and June surveys, as well as Total Count gamma-ray data, because these variables provide independent information for a similar shallow exploration depth. Independency was tested by means of principle component analysis (PCA), in which all variables were included. Results of PCA are shown in Table 2. For the *k*-means cluster algorithm, Mahalanobis distance was used as a metric for the measuring distance of data, as it takes the different scales of input variables into account. Cluster analysis was applied on re-gridded data with a 5-m raster that were generated from the kriging interpolation maps shown in Figs. 2 and 4.

A critical issue when utilizing the zonal approach is the choice of optimum number of clusters, which is usually specified by a priori information, data analysis using, e.g. cross plots, or statistical criteria. Variance ratio criterion, originally introduced by Calinski and Harabasz (1974), is a widely used criterion, which uses the quotient between the intra-cluster average squared distance and inter-cluster average squared distance. The optimal solution of this criterion is the number of clusters that maximizes the value of the variance criterion.

Based on the statistical criterion, a 2-cluster and a 5-cluster model would be appropriate results according to the input variables (Fig. 6). Zonation into only two subareas (a steeper northwest, and an eastern part), however, is not a meaningful partitioning of the hill-slope surface with regards to the spatially high-resolution geophysical measurements, as well as to further a priori information. We rely on additional information from an ecological moisture index that has been obtained from mapping indicator vegetation and soil cores from the entire catchment (Lindenmaier et al., 2005). Based on the original ecological moisture map, we can discriminates between five different classes of soil conditions for our study area, thus the 5-cluster solution appears to be an adequate zonation model for the hill-slope area. A detailed map of the classified patches of ecological plant moisture that matches the extent of geophysical mapping, as well as the partitioning of the hill-slope area according to the 5-cluster model, is shown in Fig. 7.

Both maps in Fig. 7 show a comparable pattern of hill-slope partitioning into zones of similar subsurface conditions. Based on ecological classification, the study area is characterized by very moist to very wet soil conditions with stagnic properties in plane areas, and some drier bulging areas in the steeper northwest (Lindenmaier et al., 2005). Similar conditions can be assumed for the obtained cluster partitioning, even though a detailed assessment of the qualities of the clusters is complicated by the ambiguous relationship between the measured physical parameters and the soil properties. However, at least the cluster numbers 1 and 5 can be regarded as being relatively well defined, in accordance with the characteristics of allocated data shown in Fig. 8. Thus, according to the low gamma values and their specific relation to soil-water content, cluster 1 is very likely to specify wet soil conditions analog to the dark grey area of the ecological moisture map, which is independently confirmed by the high water contents of the soil samples concerned (Fig. 8b). Secondly, cluster 5 matches the extent of the area categorized as an artificial surface in Fig. 8a, which is in accordance with the highest gamma values interpreted as artificial backfill material. All further clusters were statistically defined and delineate similar soil conditions with variable response o EMI and gamma-ray methods.

Differences in hill-slope zonation between both maps in Fig. 8 have to be examined in the light of the very different approaches and data used for cluster partitioning. Ecological mapping is based on the tolerance range of plants to the availability of moisture and qualitative and quantitative soil properties (e.g. soil type, layer depth, organic content, and color). Given an undisturbed surface and natural vegetation, these properties describe long-term characteristics of a habitat. In contrast, geophysical methods provide a snap shot of the spatial variability of specific proxy values (physical variables) at the moment of surveying. Regardless of the different procedures, a comparable partition of the shallow hill-slope subsurface with geophysical surveying has been achieved, and demonstrated the potential for rapid surveying and assessment of soil conditions of heterogeneous and complex field sites at the intermediate landscape scale.

4 Conclusions

The combination of EMI and gamma-ray spectroscopy has proven to be a suitable approach for mapping soil proxy values rapidly at the intermediate hill-slope scale. Both

HESSD
9, 2511–2539, 2012

survey designs "on-the-go" and point measurements provided appropriate data sets for analyzing spatial variability and identifying subsurface structures by means of kriging interpolation. A quantification of soil qualities, in particular soil moisture based on the proxy values was not possible due to ambiguous relationship of electrical conductivity and gamma-ray flux to the highly heterogeneous soil conditions. Based on few soil-sample analyses, no relevant relationship was found to exist between soil moisture and EC_a for the entire test site. Gamma-ray emissions seemed to be negatively correlated with soil-water content. Even though we aimed at minimal invasive measures, it is an open question for further field tests, if more samples or more detailed laboratory analyses, e.g. particle size analysis, could establish more reliable and significant relationships between proxy and soil state variables at such heterogeneous field sites.

However, despite the uncertainties of the applied methods, we obtained valuable information on soil conditions by qualitative analyses of the proxy values. Based on EMI measurements, we revealed the relative variability of EC_a from two different depth intervals that showed an increased spatial and vertical heterogeneity of distinct soil conditions in May, compared to more smoothed EC_a pattern in June. Since temporal changes in EC_a can be very likely related to relative changes in soil-moisture content, repeated EMI measurements can potentially be used for qualitative soil-moisture monitoring at complex hill-slope sites. Emission data obtained from a single gamma-ray survey seemed to be closer related to soil-moisture, as shown by the notable correlation between Total Count and K results with gravimetric water contents. Besides a relative monitoring, it appears possible to implement a semi-quantification of soil-water contents based on repeated gamma-ray measurements together with few samples for obtaining water contents of clayey soils. Finally, the results of both EMI and gamma-ray methods enabled a meaningful partitioning of hill-slope subsurface into zones of similar subsurface conditions that was in exceptionally good agreement with the previously obtained hill-slope partitioning based on ecological factors. Therefore we believe that qualitative, but area-wide information on soil conditions based on proxy values are very useful for a primary exploration of larger study areas prior to more detailed

HESSD
9, 2511–2539, 2012

investigations in terms of implementing a hierarchical site investigation approach for future targeted measures in relevant subareas.

Acknowledgements. The authors thank Malte Ibs-von Seht (Federal Institute for Geosciences and Natural Resources, BGR, Germany) for providing the gamma-ray spectrometer and David Sauer (University of Potsdam, Germany) for his assistance during fieldwork. This work was funded by Deutsche Forschungsgemeinschaft as part of the research unit "Coupling of flow and Deformation processes for modeling the movement of natural slopes (DFG research unit 581).

References

Altdorff, D. and Dietrich, P.: Combination of electromagnetic induction (EMI) and gamma-spectrometry using *k*-means clustering: A study for evaluation of site partitioning, J. Plant Nutr. Soil Sc., in press, 2012.

Brevik, E. C., Fenton, T. E., and Lazari, A.: Soil electrical conductivity as a function of soil water content and implications for soil mapping, Precis. Agric., 7, 393–404, 2006.

Buchanan, S. and Triantafilis, J.: Mapping Water Table Depth Using Geophysical and Environmental Variables, Ground Water, 47, 80–96, 2009.

Calinski, T. and Harabasz, J.: A dendrite method for cluster analysis, Commun. Stat., 3, 1–27, 1974.

Carroll, T. R: Airborne soil moisture measurements using natural terrestrial gamma radiation, Soil Sci., 132, 358–366, 1981.

Carroll, Z. L. and Oliver, M. A.: Exploring the spatial relations between soil physical properties and apparent electrical conductivity, Geoderma, 128, 354–374, 2005.

Chambers, J. E., Wilkinson, P. B., Kuras, O., Ford, J. R., Gunn, D. A., Meldrum, P. I., Pennington, C. V. L., Weller, A. L., Hobbs, P. R. N., and Ogilvy, R. D.: Three-dimensional geophysical anatomy of an active landslide in Lias Group mudrocks, Cleveland Basin, UK, Geomorphology, 125, 472–484, 2011.

Cockx, L., M., Van Meirvenne, and De Vos, B.: Using the EM38DD Soil sensor to delineate clay lenses in a sandy forest soil, Soil Sci. Soc. Am. J., 71, 1314–1322, 2007.

Cook, S. E., Corner, R. J., Groves, P. R., and Grealish, G. J.: Use of airborne radiometric data for soil mapping, Aust. J. Soil Res., 34, 183–194, 1996.

HESSD

9, 2511–2539, 2012

Corwin, D. L. and Lesch, S. M.: Application of Soil Electrical Conductivity to Precision Agriculture: Theory, Principles, and Guidelines, Agron. J., 95, 455–471, 2003.
Corwin, D. L., Kaffka, S. R., Hopmans, J. W., Mori, Y., van Groenigen, J. W., van Kessel, C., Lesch, S. M., and Oster, J. D.: Assessment and field-scale mapping of soil quality properties of a saline sodic soil, Geoderma, 114, 231–259, 2003.
Depenthal, C. and Schmitt, G.: Monitoring of a landslide in Vorarlberg/ Austria, in: Proc. Int. FIG Symp. on Deformation Measurements, 11th, Santorini (Thera) Island, Greece, edited by: Stiros, S. and Pytharouli, S., 289–295, 2003.
Dickson, B. L. and Scott, K. M.: Interpretation of aerial gamma ray surveys-adding the geochemical factors, AGSO Journal of Australian Geology & Geophysics, 17, 187–200, 1997.
Dietrich, P. and Tronicke, J.: Integrated analysis and interpretation of cross-hole P- and S-wave tomograms: a case study, Near Surf. Geophys., 7, 101–109, 2009.
Domsch, H. and Giebel, A.: Estimation of soil textural features from soil electrical conductivity recorded using the EM38, Precis. Agric., 5, 389–409, 2004.
Ewing, R. P. and Hunt, A. G.: Dependence of the Electrical Conductivity on Saturation in Real Porous Media, Vadose Zone J., 5, 731–741, 2006.
Grasty, R. L.: Radon emanation and soil moisture effects on airborne gamma-ray measurements, Geophysics, 62, 1379–1385, 1997.
IAEA: Guidelines for radioelement mapping using gamma ray spectrometry data, I. A. E. Agency, Vienna, Austria, International Atomic Energy Agency, 2003.
Kachanoski, R. G., Gregorich, E. G., and van Wesenbeeck, I. J.: Estimating spatial variations of soil water content using noncontacting electromagnetic inductive methods, Can. J. Soil Sci., 68, 715–722, 1988.
Kachanoski, R. G., de Jong, E., and van Wesenbeeck, J.: Field scale patterns of soil water storage from non-contacting measurements of bulk electrical conductivity, Can. J. Soil Sci., 70, 527–541, 1990.
Kiss, J. J., De Jong, E., and Bettany, J. R.: The distribution of natural radionuclides in native soils of southern Saskatchewan, Canada, J. Environ. Qual., 17, 437–445, 1988.
Lindenmaier, F., Zehe, E., Dittfurth, A., and Ihringer, J.: Process identification at a slow-moving landslide in the Vorarlberg Alps, Hydrol. Process., 19, 1635–1651, 2005.
Martínez, G., Vanderlinden, K., Giráldez, J. V. Espejo, A. J., and Muriel, J. L.: Field-Scale Soil Moisture Pattern Mapping using Electromagnetic Induction, Vadose Zone J., 9, 871–881, 2010.

HESSD
9, 2511–2539, 2012

Assessment of shallow subsurface characterization

S. Popp et al.

McNeill, J. D.: Electrical conductivity of soils and rocks, Technical Note TN-5, Geonics Ltd. Mississauga, Ontario, 22 p., 1980.
Minty, B.: Fundamentals of airborne gamma-ray spectrometry, AGSO Journal of Australian Geology & Geophysics, 17, 39–50, 1997.
Paasche, H., Tronicke, J., and Dietrich, P.: Automated integration of partially colocated models: Subsurface zonation using a modified fuzzy c-means cluster analysis algorithm, Geophysics, 75, P11–P22, 2010.
Pracilio, G., Adams, M. L., Smettem, K. R. J., and Harper, R. J.: Determination of spatial distribution patterns of clay and plant available potassium contents in surface soils at the farm scale using high resolution gamma ray spectrometry, Plant Soil, 282, 67–82, 2006.
Reedy, R. C. and Scanlon, B. R.: Soil Water Content Monitoring Using Electromagnetic Induction, J. Geotech. Geoenviron., 129, 1028–1039, 2003.
Robinson, D. A., Lebron, I., Kocar, B., Phan, K., Sampson, M., Crook, N., and Fendorf, S.: Time-lapse geophysical imaging of soil moisture dynamics in tropical deltaic soils: An aid to interpreting hydrological and geochemical processes, Water Resour. Res., 45, W00D32, doi:10.1029/2008WR006984, 2009.
Robinson, D. A., Abdu, H., Lebron, I., and Jones, S. B.: Imaging of hill-slope soil moisture wetting patterns in a semi-arid oak savanna catchment using time-lapse electromagnetic induction, J. Hydrol., 419–417, 39–49, 2012.
Sass, O., Bell, R., and Glade, T.: Comparison of GPR, 2D-resistivity and traditional techniques for the subsurface exploration of the Oschingen landslide, Swabian Alb (Germany), Geomorphology, 93, 89–103, 2008.
Schneider, U.: Untersuchungen zur Kinematik von Massenbewegungen im Modellgebiet Ebnit (Vorarlberger Helvetikum), Diss. Univ. Karlsruhe, Karlsruhe, Germany, 1999.
Schrott, L. and Sass, O.: Application of field geophysics in geomorphology: Advances and limitations exemplified by case studies, Geomorphology, 93, 55–73, 2008.
Sheets, K. R. and Hendrickx, J. M. H.: Noninvasive soil water content measurement using electromagnetic induction, Water Resour. Res., 31, 2401–2409, 1995.
Sherlock, M. D. and McDonnell, J. J.: A new tool for hillslope hydrologists: spatially distributed groundwater level and soilwater content measured using electromagnetic induction, Hydrol. Process., 17, 1965–1977, 2003.
Taylor, M. J., Smettem, K., Pracilio, G., and Verboom, W.: Relationships between soil properties and high-resolution radiometrics, central eastern Wheatbelt, Western Australia, Explor.

HESSD
9, 2511–2539, 2012

Assessment of shallow subsurface characterization

S. Popp et al.

Geophys., 33, 95–102, 2002.
Tromp-van Meerveld, H. J. and McDonnell, J. J.: Assessment of multi-frequency electromagnetic induction for determining soil moisture patterns at the hillslope scale, J. Hydrol., 368, 56–67, 2009.
Tronicke, J., Holliger, K., Barrash, W., and Knoll, M. D.: Multivariate analysis of crosshole georadar velocity and attenuation tomograms for aquifer zonation, Water Resour. Res., 40, W01519, doi:10.1029/2003WR002031, 2004.
Van Dam, R. L.: Landform characterization using geophysics–Recent advances, applications, and emerging tools, Geomorphology, 137, 57–73, 2012.
Viscarra Rossel, R. A., Taylor, H. J., and McBratney, A. B.: Multivariate calibration of hyperspectral γ-ray energy spectra for proximal soil sensing, Eur. J. Soil Sci., 58, 343–353, 2007.
Wienhofer, J., Lindenmaier, F., and Zehe, E.: Challenges in Understanding the Hydrologic Controls on the Mobility of Slow-Moving Landslides, Vadose Zone J., 10, 496–511, 2011.
Wilford, J. R., Bierwirth, P. N., and Craig, M. A.: Application of airborne gamma-ray spectrometry in soil/regolith mapping and applied geomorphology, AGSO Journal of Australian Geology & Geophysics, 17, 201–216, 1997.

HESSD
9, 2511–2539, 2012

Assessment of shallow subsurface characterization

S. Popp et al.

Table 1. Descriptive statistics of EMI measurements (in $mS\,m^{-1}$) in horizontal (EC_h) and vertical (EC_v) dipole configuration and gamma-ray spectroscopy (in counts per 60 s). SD: standard deviation, CV: coefficient of variation [(SD/Mean)*100].

	EC_h May	EC_v May	EC_h June	EC_v June	γK	γU	γTh	γTotal Count
Mean	37.1	26.7	31.3	30.4	226	60	36	1230
Min	17.0	1.0	11.8	10.4	44	13	11	393
Max	57.3	52.2	56.5	60.1	583	125	83	2537
SD	6.4	8.0	7.0	8.2	85	17	12	346
CV (%)	17.3	30.0	22.4	27.0	37.6	28.3	33.3	28.1

Table 2. Results of the PCA: the Component Loadings shows the variance of each variable explained by three factors. Maximum variances of the selected variables for cluster analysis are explained by different factors (italic). Below the respective percentage of the three factors which explain altogether 92 % of total variance.

Component Loadings	1	2	3
EC_h May	0.358	0.412	*−0.833*
EC_v May	−0.692	0.484	−0.101
EC_h June	−0.016	*0.935*	0.153
EC_v June	−0.588	0.740	0.244
γTotal Count	*0.976*	0.162	0.087
γK	0.969	0.148	0.084
γU	0.916	0.214	0.136
γTh	0.955	0.147	0.087
Total variance explained (%)	57.44	24.26	10.35

HESSD
9, 2511–2539, 2012

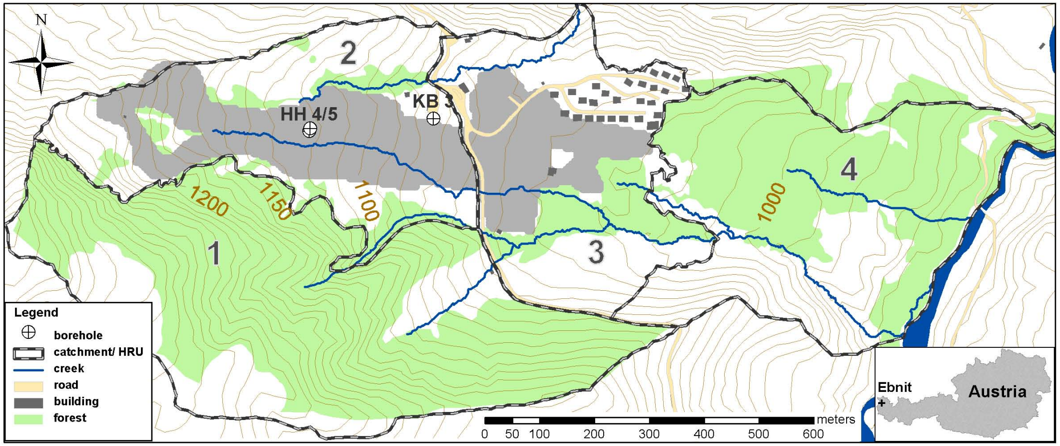

Fig. 1. Topography of the Heumöser catchment near Ebnit (Vorarlberg, Austria). The grey-shaded region indicate the open meadow area, on which geophysical mapping was focused. Numbers 1 to 4 indicate the major hydrologic units (HRU).

HESSD
9, 2511–2539, 2012

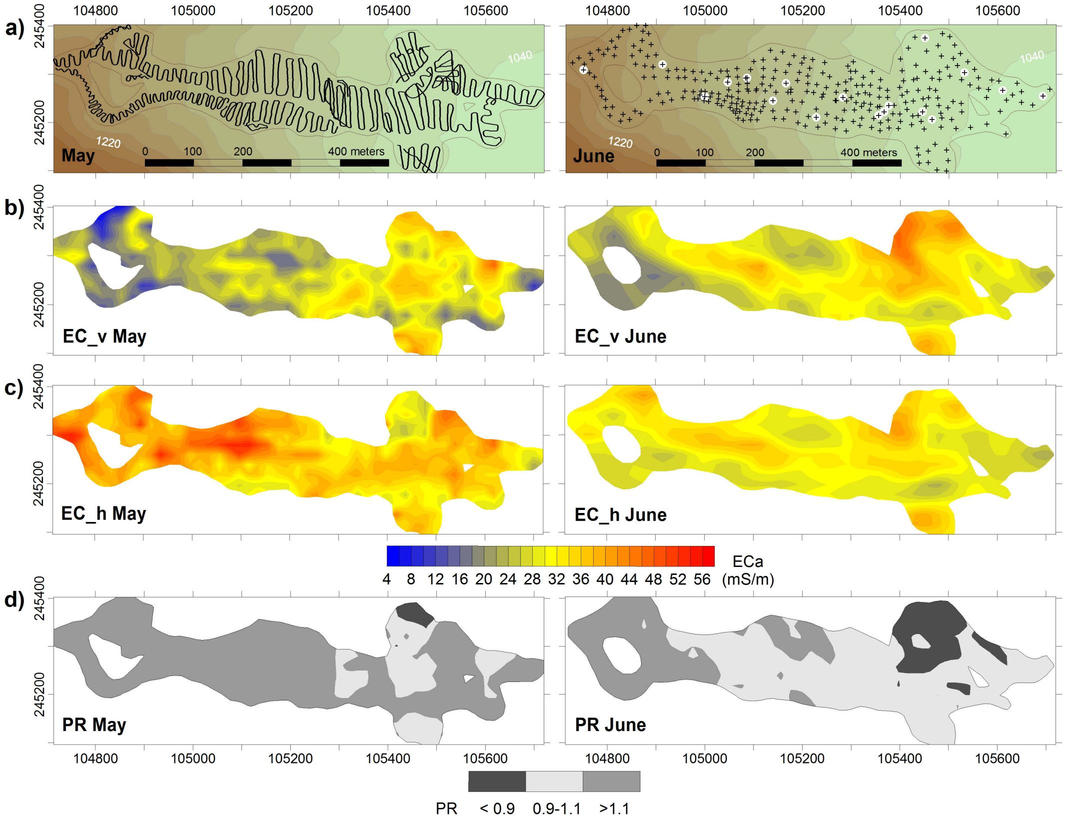

Fig. 2. EMI measurements from May (left column) and June (right column) with different survey designs and location of reading points **(a)**. White dots in the map on the right show soil sampling locations. The detail views show maps obtained by block ordinary kriging of EC_a ($mS\,m^{-1}$) using **(b)** the vertical (EC_v) and **(c)** the horizontal dipole orientation (EC_h), as well as **(d)** the profile ratio (PR). Coordinates on x and y axis are in metric BMN M28 Austrian coordinate system.

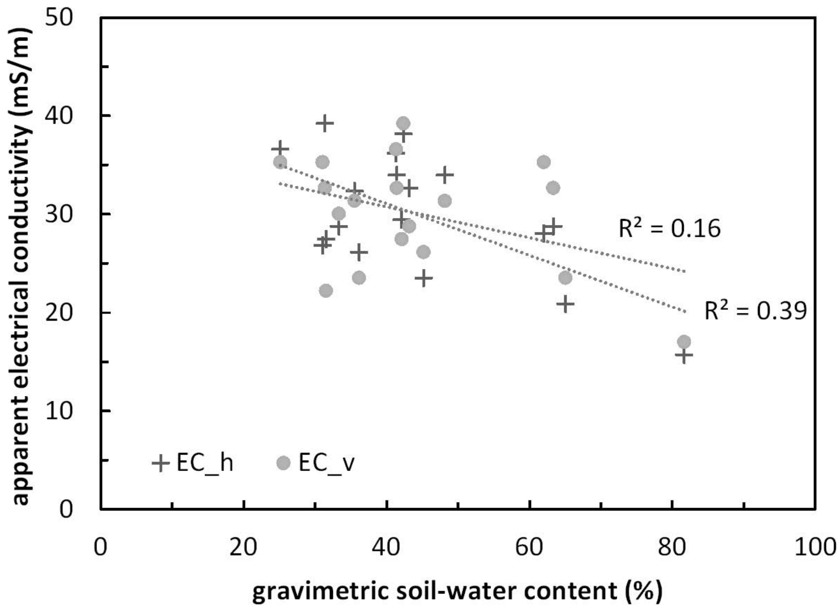

Fig. 3. Scatterplot of gravimetric soil-water content and EC_a data, seperated into EC_h and EC_v according to the respective sensor orientation in June survey.

HESSD
9, 2511–2539, 2012

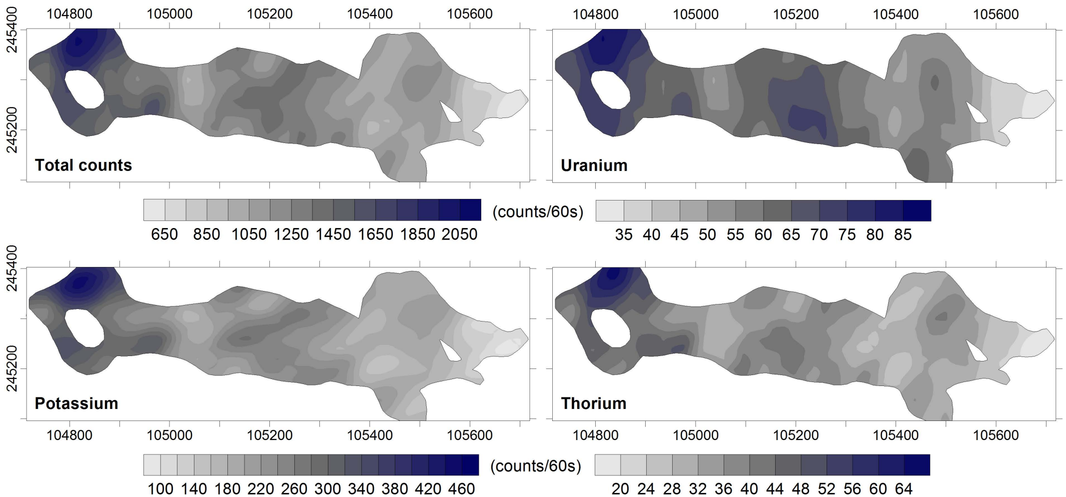

Fig. 4. Maps of interpolated gamma radiation (in counts per 60 s) using individual data of Total Count (top left), potassium or K (on the left at the bottom) uranium or U (top right), and thorium or Th (on the right at the bottom). Note the different scales of data ranges. Coordinates on x and y axis are in metric BMN M28 Austrian coordinate system.

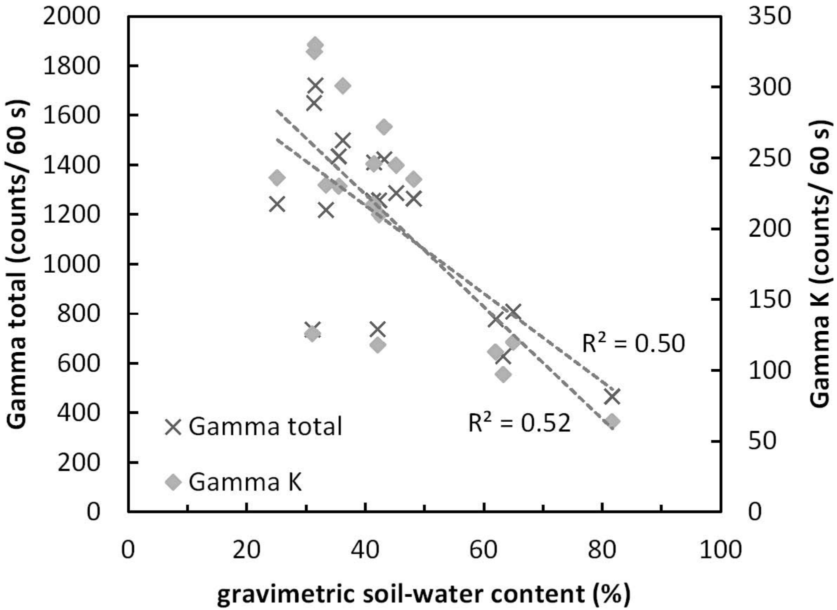

Fig. 5. Scatterplot of gravimetric soil-water content and total gamma counts (left axis) and radioaktive K (right axis).

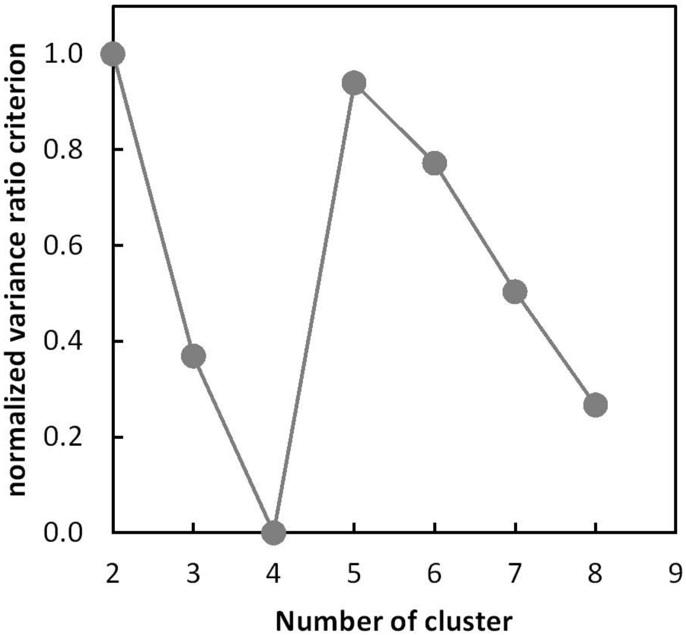

Fig. 6. Normalized variance ratio criterion as a function of the optimum number of clusters.

HESSD

9, 2511–2539, 2012

Assessment of shallow subsurface characterization

S. Popp et al.

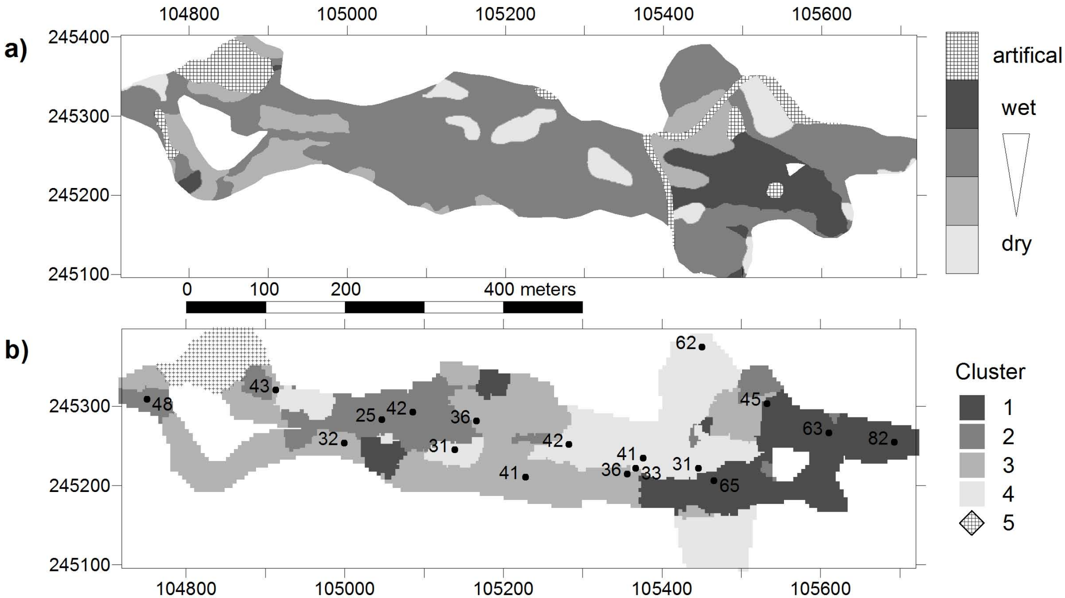

Fig. 7. Detail map of hill-slope partitioning based on **(a)** the ecological zonation based on Lindenmaier et al. (2005), and **(b)** the 5-cluster model with locations of the soil samples. The numbers denote the determined soil-water contents. The different shades of grey in both maps indicate the different ecological classes and clusters, respectively. Coordinates on x and y axis are in metric BMN M28 Austrian coordinate system.

HESSD
9, 2511–2539, 2012

Assessment of shallow subsurface characterization

S. Popp et al.

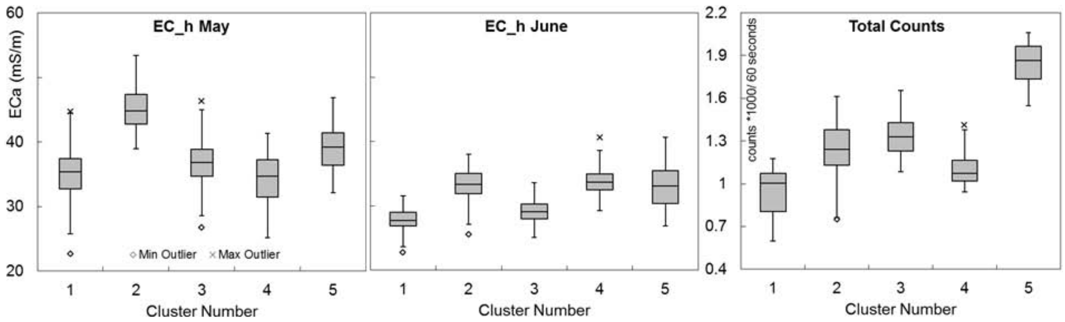

Fig. 8. Characteristics of input variables in the respective clusters. The top and bottom of the boxes indicate the upper and lower quartile, the line inside refers to the median value. Whiskers define the data range within the 1.5 IQR (interquartile range), and values off the IQR are given as outliers. Note the different scales of the y axis between EC_a and gamma data plots.